Semiconductors, Vol. 37, No. 7, 2003, pp. 832–837. Translated from Fizika i Tekhnika Poluprovodnikov, Vol. 37, No. 7, 2003, pp. 860–865.

CONFERENCE. PHYSICS OF SEMICONDUCTOR DEVICES

Splitting of Resonant Optical Modes in Fabry–Perot Microcavities

V. G. Golubev, A. A. Dukin*, A. V. Medvedev, A. B. Pevtsov, A. V. Sel'kin, and N. A. Feoktistov

Ioffe Physicotechnical Institute, Russian Academy of Sciences, Politekhnicheskaya ul. 26, St. Petersburg, 194021 Russia

**e-mail: dookin@gvg.ioffe.rssi.ru*

Submitted December 23, 2002; accepted for publication December 27, 2002

Abstract—Splitting of resonant optical modes in Fabry–Perot microcavities with distributed Bragg reflectors is studied experimentally. The splitting was detected in polarized light at large angles of incidence onto the external boundary of a microcavity. A theoretical model is developed which makes it possible to describe quantitatively all of the special features of the splitting observed. *© 2003 MAIK "Nauka/Interperiodica".*

INTRODUCTION

Recently, much attention has been focused on Fabry–Perot microcavities (MCs) because of their interesting physical properties [1]. Some examples of the phenomena that were observed in MCs are given by Rabi splitting due to the interaction of localized optical modes with excitons in quantum wells [2], the splitting of eigenmode frequencies in a system of two MCs coupled by a common mirror [3], and the polarization splitting of eigenfrequencies of optical TM and TE modes [4]. Most of the effects in MCs were studied at angles close to normal incidence of light.

The aim of this study is a detailed investigation of the optical eigenmode of a planar MC at large angles of incidence. As experimental samples, we used MCs on the basis of oxygen-saturated hydrogenated amorphous silicon (*a*-SiO_x:H) and tin oxide (SnO_x). The splitting of the optical-mode resonant frequency in one of the polarizations of light is revealed. The value of splitting and the polarization (TM or TE) in which it appears depend on the optical constants of the individual layers and the MC geometry.

EXPERIMENTAL

The microcavity under consideration is a thin-film structure comprised of alternating layers of oxygen-saturated hydrogenated amorphous silicon (*a*-SiO_x:H) and tin oxide (SnO_x).[1] A schematic of the MC structure is shown in Fig. 1. The upper (*A*) and the lower (*B*) distributed Bragg reflectors (DBRs) consist of two pairs of quarter-wave layers of SnO_x and *a*-SiO_x:H (the respective thicknesses are $\lambda/4n_1$ and $\lambda/4n_2$) with a high (n_1) and a low (n_2) refractive indices ($n_1 = 1.87$ for SnO_x and $n_2 = 1.46$ for *a*-SiO_x:H). A half-wave active layer of SnO_x with the thickness $\lambda/2n_1$ is placed between the two DBRs. The optical parameters of the layers were determined from the interference pattern recorded directly during the growth of the microcavity structure. The properties of each layer were independently obtained from ellipsometry measurements. The thicknesses of the layers were chosen so that the resonance wavelength (λ) in vacuum at normal incidence of light

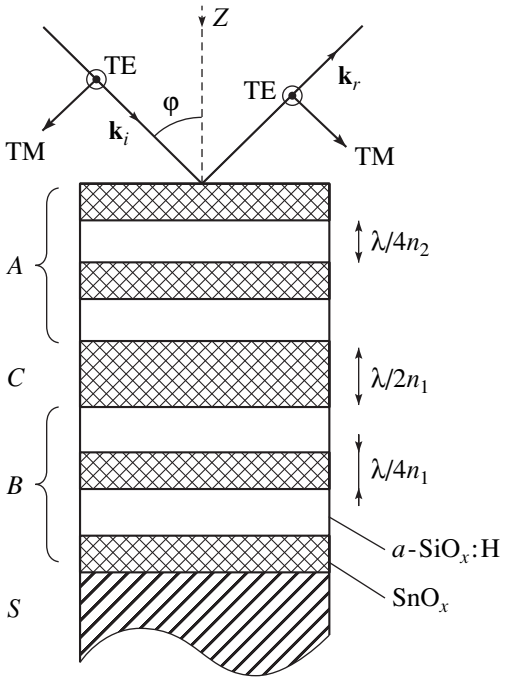

Fig. 1. Scheme of an SnO_x/*a*-SiO_x:H-based microcavity consisting of two quarter-wave distributed Bragg reflectors, the upper (*A*) and the lower (*B*), and a half-wave active SnO_x layer (*C*). *S* is the quartz substrate; $\mathbf{k}_i$ and $\mathbf{k}_r$ are the wave vectors of the incident and reflected waves, respectively; φ is the angle of light incidence; TM and TE are the polarizations of light; n_1 and n_2 are the refractive indices; and λ is the operating wavelength of the microcavity.

[1] The detailed description of the MC design and fabrication process are given in [5–9].

1063-7826/03/3707-0832$24.00 © 2003 MAIK "Nauka/Interperiodica"

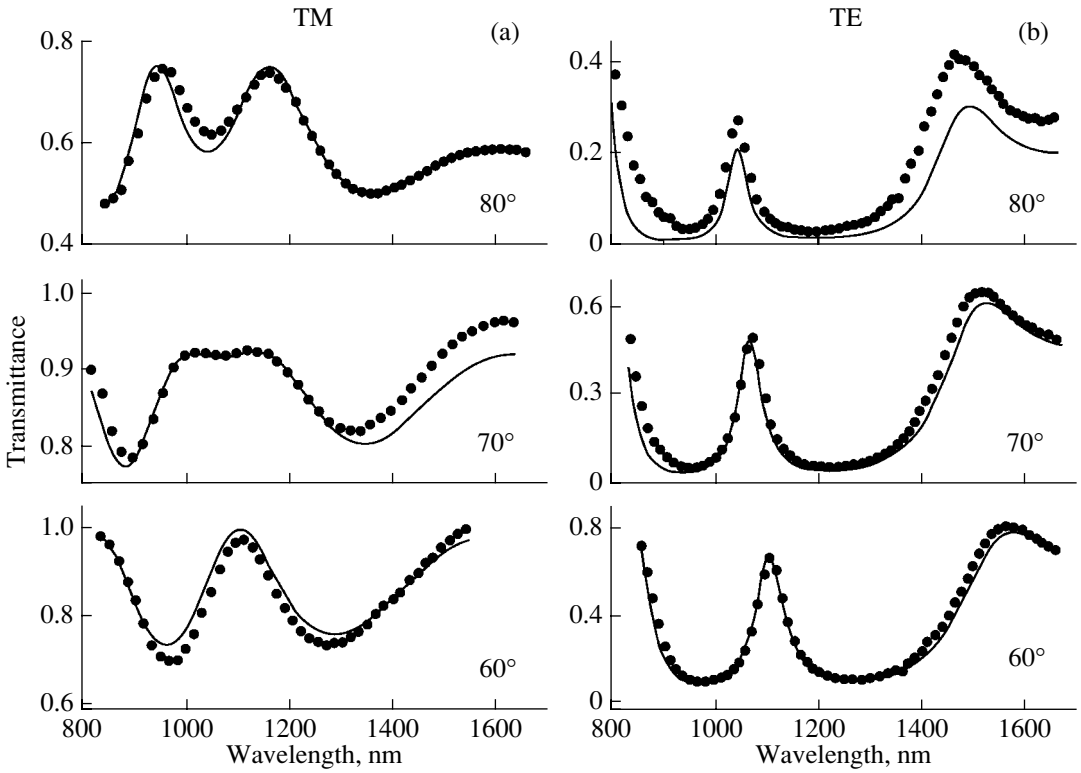

Fig. 2. Transmission spectra of the SnO_x/a-SiO_x:H-based microcavity at the angles of incidence φ = 60°, 70°, and 80° for (a) TM and (b) TE polarizations. Circles show the experimental results and solid curves show the results of calculations.

lies within the range from 1.3 to 1.5 μm, which corresponds to the range used by modern fiber-optics communication devices.

The materials of the layers were selected so that the microcavity structure grown had a fairly high optical contrast $2(n_1 - n_2)/(n_1 + n_2)$, which allows one to observe the MC eigenmodes with a minimum number of periods within DBR. The latter circumstance plays an important role in simplifying the technological process of growing a multilayer structure.

Spectroscopic studies were carried out using a computer-controlled grating monochromator equipped with an InGaAs-based photodiode as a radiation detector. We performed the measurements in the synchronous-detection mode. The transmission signal was collected from the surface area of 1 mm^2. The angular aperture did not exceed 0.7° during the measurements, which enabled us to avoid undesirable broadening of resonance lines as a result of collimation of beams passed through the MC at different angles.

We measured the MC transmission spectra both in TM and TE polarizations at different angles of incidence in the range from 0° to 85°. The spectra were recorded in the interval including the value corresponding to the photonic band gap [1]. As long as the angle of incidence is no greater than 70°, the spectrum shows a clearly pronounced resonance peak, which is attributed to the excitation of an MC eigenmode. At larger angles, a doublet structure of the resonance peak appears in TM polarization; whereas, in TE polarization, such a structure is absent at any angle of light incidence.

The MC transmission spectra in the region of the photonic band gap is shown by dotted curves in Fig. 2 for (a) TM and (b) TE polarizations and three angles of incidence (φ = 60°, 70°, and 80°). It is seen that, in TM polarization, the doublet structure is absent at φ = 60°, arises at 70°, and becomes pronounced at 80°. The splitting of the doublet increases with increasing φ. In TE polarization, only one resonance peak is detected at the same angles of incidence. The TE peak turns out to be narrower than the TM peak. The photonic band gap most clearly manifests itself in TE polarization as an appreciable increase in the transmission coefficient at the long- and the short-wavelength edges of the spectral range considered.

Dots in Fig. 3 show the spectral position of the experimental resonance peaks versus the angle of light incidence. As the angle increases, the resonance wavelength corresponding to the maximum transmission decreases. For angles ranging from 0° to 70°, the resonance frequencies for TM and TE polarizations coincide. At the angles exceeding 70°, a distinct splitting of the resonance peak is observed in TM polarization. It should be noted that the appearance of the splitting is threshold-like.

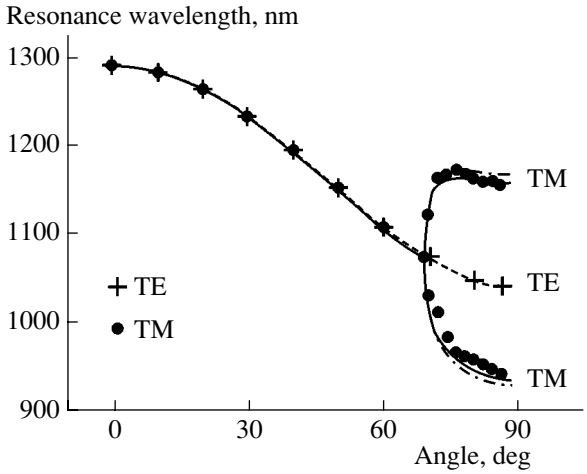

Fig. 3. Angular dependence of the resonance wavelengths of the SnO_x/a-SiO_x:H-based microcavity for TM and TE polarizations. Circles represent the experimental results. Solid and dashed curves show the wavelengths of the resonance transmission peaks obtained from the spectra calculated by the transfer-matrix method for TM and TE polarizations, respectively. The dot-and-dash line is the result of calculating TM polarization according to analytical expression (3).

In order to explain the experimental results, in what follows, we suggest a model for the formation of transmission spectra of an MC structure at large angles of light incidence.

THEORETICAL MODEL

The transmission spectra of the structure studied were calculated by the transfer-matrix method [10]. The calculated spectra (solid curves in Fig. 2) were fitted to the experimental data by varying the refractive index of SnO_x and the MC layers' thickness. As can be seen, good agreement between the theoretical and the experimental results was achieved. The calculated curves reproduce all the special features of the experimental spectra including the photonic band gap and the resonance peak with its doublet structure.

The resonance wavelengths providing for the maximum transmission through the studied MC structure ($n_1 > n_2$) versus the angle of light incidence were derived from the calculated spectra for TM polarization (solid line in Fig. 3) and TE polarization (dashed line). The calculated values correlate well with the experiment. The resonance wavelength decreases with increasing angle of incidence. For angles in the range from 0° to 70°, the resonance wavelengths for both polarizations are very close (small polarization splitting [11]). This fact is attributed to the relatively low value of the optical contrast, as well as to the fact that the optical thicknesses of the DBR layers and the active layer are equal to $\lambda/4$ and $\lambda/2$, respectively, with high accuracy.

In order to establish the reasons for TM-peak splitting, we make a number of simplifying assumptions. Let us assume the optical thickness of the active layer and that of the DBR layers to be equal to $\lambda/2$ and $\lambda/4$, respectively. The relationship between the refractive indices of the MC layers is such that, at any angle of incidence, the Brewster effect does not occur at the interfaces between the adjacent DBR layers ($n_V > 1/\sqrt{n_1^2 + n_2^2}$, where n_V is the refractive index of the external medium).

Analysis shows that, under certain conditions, a constructive interference of waves (summation of waves with the same phase) in the region of the photonic band gap occurs at the internal boundaries of the external quarter-wave layer of the upper DBR (this layer is adjacent to the external medium). For TE polarization, such interference occurs at any angle of light incidence if $n_1 < n_2$ (see the arrangement of layers in Fig. 1). In TM polarization, the interference becomes constructive if $n_1 > n_2$ and the angle of incidence φ exceeds the Brewster angle $\varphi_{Br} = \arctan(n_1/n_V)$ or if $n_1 < n_2$ and $\varphi < \varphi_{Br}$. For angles of incidence close to 90°, the reflectivity at the upper boundary of the external layer tends to unity, which results in the formation of an additional MC denoted as $MC_{\lambda/4}$, in contrast to $MC_{\lambda/2}$ in the half-wave active layer. Thus, at large angles of incidence, we obtain a system of two MCs coupled by a common two-sided mirror, which is formed by the part of the upper DBR between the active and the upper (external) layers.

It is known that, in a system of two MCs coupled by a common mirror, the frequencies of eigenmodes may split [11]. Similar splitting should also be expected in the system under study.

In the region of the photonic band gap, the energy reflection coefficient of a DBR $R_{DBR} = |r_{DBR}|^2$ is nearly frequency-independent. The phase of the amplitude reflection coefficient r_{DBR} varies nearly linearly [8, 11]:

$$r_{DBR}^{\sigma} = \pm\sqrt{R_{DBR}^{\sigma}}\exp\{i\alpha^{\sigma}(\varphi)[\omega - \bar{\omega}^{\sigma}(\varphi)]\},$$

where σ = TM, TE denotes polarization, φ is the angle of incidence in the external medium, $\alpha^{\sigma}(\varphi)$ is the proportionality factor between the phase and frequency, and $\bar{\omega}^{\sigma}(\varphi)$ is the "central" frequency of the photonic band gap. The coefficient $\alpha^{\sigma}(0)$ is inversely proportional to the difference between the refractive indices:

$$\alpha^{\sigma}(0) \equiv \alpha(0) = \bar{\lambda}n_1n_2/[2c(n_1 - n_2)n],$$

where $\bar{\lambda} = 2\pi c/\bar{\omega}(0)$, c is the speed of light, n is the refractive index of the medium from which the wave falls on a DBR, and $\bar{\omega}(0) \equiv \bar{\omega}^{TM}(0) = \bar{\omega}^{TE}(0)$ [12]. The phase of the amplitude reflection coefficient at the frequency $\bar{\omega}^{\sigma}(\varphi)$ is equal to zero (sign "+") if $n \geq n_1, n_2$ and to π (sign "–") if $n \leq n_1, n_2$.

The amplitude transmission coefficient t_{MC} of a microcavity as a whole is described by the following expression (from here on, we omit the index σ, which denotes polarization):

$$t_{MC} = \frac{t_{top}t_{com}\Phi^{3/2}t_{BB}t_{SV}}{1-\tilde{r}_{top}r_{com}\Phi-\tilde{r}_{com}r_B\Phi^2+\tilde{r}_{top}r_B\Phi^3\tilde{r}_{com}/r^*_{com}}, \quad (1)$$

where t_{BB} and r_B are the amplitude coefficients of transmission and reflection of light of the DBR B in the case of incidence of light from the side of the active layer; t_{SV} is the amplitude transmission coefficient at the substrate–external-medium interface; $\Phi = \exp(i\beta\omega)$ determines the phase increment of the wave as it passes through an active layer with the thickness L_c, $\beta = L_c\sqrt{n_1^2 - n_x^2}/c$, $n_x = n_V\sin\varphi$; t_{com} and r_{com} are the amplitude coefficients of transmission and reflection of a common mirror placed in a medium with the refractive index n_1; t_{top} and $\tilde{r}_{top}$ are the amplitude coefficients of transmission and reflection at the interface between the external layer of the upper DBR (A) and the external medium. Symbol "~" indicates that the wave propagation is opposite the Z axis.

Analysis of the poles of expression (1) in the approximation $\arg r_B \approx \arg r_{com}$ (which is confirmed by exact numerical calculations) indicates the existence of a critical angle of incidence φ_{Sp}; exceeding this angle results in the splitting of the eigenmode frequencies. An approximate analytical expression for φ_{Sp} is given in the Appendix.

With the use of (1), the MC transmission spectrum in the region of the photonic band gap can be thought of as the product of three resonance factors:

$$T_{MC} = \frac{A}{|x-x_1|^2|x-x_2|^2|x-x_3|^2}, \quad (2)$$

where $x = \exp\{i[(\alpha+\beta)\omega - \alpha\bar{\omega}]\}$ and A and $x_{1,2,3}$ are the constants governed by the MC parameters (see Appendix).

The analytical expression for the splitting of the resonance transmission peak $\Delta\omega_r$ obtained on the basis of formula (2) is presented in the Appendix. The frequencies of the two resonance peaks $\omega_{r_{1,2}}$ are determined as

$$\omega_{r_{1,2}} = \omega_0 \pm \Delta\omega_r/2, \quad (3)$$

where $\omega_0 = (\alpha\bar{\omega} + \pi)/(\alpha + \beta)$ is the resonance frequency for uncoupled $MC_{\lambda/2}$ and $MC_{\lambda/4}$, i.e., when $|r_{com}| = 1$.

The resonance-peak splitting arises either in TM or TE polarization, depending on whether the refractive index of the material of the external DBR layer is greater or smaller than that of the other material composing the DBR structure. Irrespective of the polarization type, the splitting is described by the same formulas (1)–(3) presented in this section and by formula (A.1) in the Appendix.

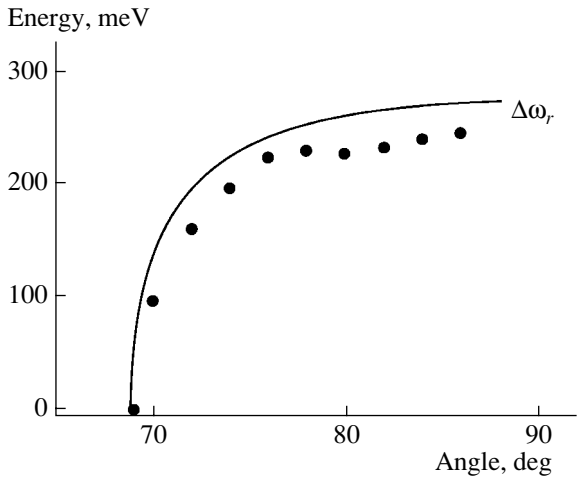

Fig. 4. Angular dependence of the TM-peak splitting for the SnO_x/a-SiO_x:H-based microcavity. Circles show the experimental data, and the solid line is the result of calculation by formula (A1).

The case considered is essentially different from that analyzed in [11] for the system consisting of two identical MCs coupled by a common internal DBR and sandwiched between two identical external DBRs. In the case under consideration, the system of two MCs is substantially asymmetric since the role of one of the external DBRs is played by the interface between the external layer of the microcavity structure and the external medium. The phase of the amplitude reflection coefficient of this interface is frequency-independent, and the reflection coefficient differs from that of the lower DBR. Furthermore, the thicknesses of the active layers in these two MCs differ by a factor of 2. This asymmetry controls the new characteristic features of the splitting, which will be discussed in the following section.

DISCUSSION

Figures 3 and 4 show the results of calculation in terms of the analytical model suggested in Section 3 in comparison with the experimental data. The spectral position of the TM-doublet components was determined from expression (3) with the use of the values $|r_{com}|$, $|r_B|$, $\bar{\omega}$, and α calculated by the transfer-matrix method. The theoretical curve in Fig. 3 (dot-and-dash line) closely correlates with the experimental points and with the results of calculation by the transfer-matrix method. When the angle of incidence is close to 70°, the splitting of the resonance peak manifests itself both in theory and experiment. Thus, the analytical model suggested allows one to interpret the observed splitting of the resonance peak as the splitting of the MC eigenmode frequencies, which arises at large

angles of incidence due to the interaction between two MCs: one in the active layer and the other in the external layer of the upper DBR.

The splitting of the resonance TM peak versus the angle of light incidence is shown in Fig. 4 (circles are the experimental data; the solid curve represents the results of calculation by formula (A.1)). The splitting process is of a threshold type. At the angles exceeding 80°, the splitting only slightly increases with increasing angle of incidence.

The splitting $\Delta\omega_r$ is governed by two parameters: the transmission coefficient t_{com} and the reflection coefficient $\tilde{r}_{top}$ under the condition that $|r_B| \approx 1$ (see Section 3). The common mirror mixes two degenerate modes of the system consisting of $MC_{\lambda/2}$ and $MC_{\lambda/4}$, thus lifting the frequency degeneracy of the modes. The transmission coefficient t_{com} controls the degree of interaction between the two modes and the value of splitting [11]. In the region $\varphi > \varphi_{Sp}$, this coefficient only slightly varies with the angle of incidence and the splitting increases mainly due to the increase in the coefficient of reflection of the interface between the upper DBR and the external medium $\tilde{r}_{top}$.

An important parameter is the minimum angle of light incidence at which the splitting of the resonance TM peak is initiated. This threshold angle can be reduced by increasing $|\tilde{r}_{top}|$ and decreasing $|r_{com}|$, which is achieved by reducing the refractive index n_1 of the DBR external layer.

The calculation of spectra by the transfer-matrix method shows that the reflection coefficient of the lower DBR $|r_B|^2$ has only a slight influence both on the threshold angle φ_{Sp} at which the splitting appears and on the value of splitting $\Delta\omega_r$ (if $|r_B|^2$ is larger than the reflection coefficient of the upper DBR). With an increase in the reflectivity of the common mirror, $\Delta\omega_r$ decreases and φ_{Sp} increases. The corresponding variation in the width of resonance peaks is small. The absorption of light in MC layers results in additional broadening of the resonance peaks.

The above results were taken into consideration when choosing the MC parameters (refractive indices, the number of DBR-containing layers, the active-layer thickness) so as to make the threshold angle low enough to be reliably detected in experiments.

CONCLUSION

A Fabry–Perot microcavity was fabricated on the basis of SnO_x/*a*-SiO_x:H by plasma-enhanced chemical-vapor deposition. The frequency of the resonance peak of transmission of this structure was studied experimentally as a function of the angle of light incidence in the range from 0° to 85° in TM and TE polarizations. Splitting of the resonance TM peak at large angles of incidence was revealed.

It is shown that resonance-peak splitting originates from the splitting of the eigenmode frequencies in a system of two microcavities coupled by a common mirror. The first microcavity represents an active layer. At large angles of incidence, the external layer of the distributed Bragg reflector adjacent to the external medium plays the role of the other MC. If the external layer consists of a material with the highest refractive index (from the refractive indices of the two materials comprising the distributed Bragg reflector), an external microcavity is formed only for TM polarization if the angle of incidence exceeds the Brewster angle at the interface between the external medium and the upper layer. This condition was met in the experiment. If the external layer is made of a material with a lower refractive index, an external microcavity is formed for TE polarization.

Approximate analytical expressions for the resonance-peak splitting and the threshold angle at which the splitting arises are obtained. The results of calculations by these expressions are in good agreement with the experimental data.

APPENDIX

Splitting of the Resonance Peaks in Transmission Spectra

At large angles of incidence, the DBR reflection coefficients $|r_{com}|$ and $|r_B|$ show only a weak angle dependence and may be calculated analytically using the formulas reported in [11] or by the transfer-matrix method. With reflection coefficients taken for the interval of angles where splitting is expected, one can find an approximate value of the angle φ_{Sp} at which splitting arises. In TM polarization (the refractive index of the external layer is n_1),

$$\varphi_{Sp} = \arcsin\sqrt{\frac{dn_V^2 - n_1^2}{n_V^2(d-1)}},$$

where

$$d = \left(\frac{n_1}{n_V}\right)^4\left(\frac{1+|\tilde{r}_{top}|}{1-|\tilde{r}_{top}|}\right)^2.$$

In TE polarization (the refractive index of the external layer is n_2, $n_2 < n_1$),

$$\varphi_{Sp} = \arcsin\sqrt{\frac{dn_2^2 - n_V^2}{n_V^2(d-1)}},$$

where

$$d = \left(\frac{1-|\tilde{r}_{top}|}{1+|\tilde{r}_{top}|}\right)^2.$$

For both polarizations,

$$|\tilde{r}_{\text{top}}| = \frac{1}{2\sqrt{2}}\sqrt{27\frac{|r_B|}{|r_{\text{com}}|^3} - 18\frac{|r_B|}{|r_{\text{com}}|} - |r_{\text{com}}||r_B| + |r_B|(|r_{\text{com}}|^2 - 9)^{3/2}\frac{\sqrt{|r_{\text{com}}|^2 - 1}}{|r_{\text{com}}|^3}}$$

The splitting of the resonance peaks in transmission spectra is expressed as

$$\Delta\omega_r = \frac{2}{\alpha + \beta}\arccos(g), \qquad \text{(A.1)}$$

where

$$g = (s\{-3s + a[-2 + s(a + 2s)]\} + v^2$$
$$+ a(a + 2s)v^2 - \sqrt{f})/(6(a + 2s)(s^2 + v^2)),$$
$$f = (s\{-3s + a[-2 + s(a + 2s)]\}$$
$$+ v^2 + a(a + 2s)v^2)^2 + 3(a + 2s)(s^2 + v^2)$$
$$\times((1 + s^2)[2a^2s + 6s^3 + a(7s^2 - 1)]$$
$$+ 2[a + (3 + a^2)s + 3as^2 + 2s^3]v^2 - (a + 2s)v^4),$$
$$s = u - a/3, \quad u = \frac{1}{2}\left(\frac{p/3}{\Lambda} - \Lambda\right),$$
$$v = \frac{\sqrt{3}}{2}\left(\frac{p/3}{\Lambda} + \Lambda\right), \quad \Lambda = \left(-\frac{q}{2} + \sqrt{\left(\frac{q}{2}\right)^2 + \left(\frac{p}{3}\right)^3}\right)^{1/3},$$
$$p = -\frac{a^2}{3} + b, \quad q = \frac{2}{27}a^3 - \frac{ab}{3} + c,$$

$a = -\mu|\tilde{r}_{\text{com}}|/\tilde{r}_{\text{top}}$, $b = -|r_{\text{com}}|/|r_B|$, $c = \mu/\tilde{r}_{\text{top}}|r_B|$, and μ is the sign of r_{com} at the photonic midgap. Under the condition $\arg r_{\text{com}} = \arg r_B$, the poles of expression (1) take the values $x_1 = u - a/3 - iv$, $x_2 = u - a/3 + iv$, and $x_3 = -2u - a/3$.

ACKNOWLEDGMENTS

This study was supported by the Ministry of Industry, Science, and Technology of the Russian Federation (under the program "Physics of Solid-State Nanostructures") and by the Russian Foundation for Basic Research, project no. 02-02-17601.

REFERENCES

1. *Microcavities and Photonic Band Gaps: Physics and Applications*, Ed. by J. Rarity and C. Weisbuch (Kluwer Academic, Dordrecht, 1996), NATO Adv. Study Inst. Ser., Ser. E, Vol. 324.
2. C. Weisbuch, M. Nishioka, A. Ishikawa, and Y. Arakawa, Phys. Rev. Lett. **69**, 3314 (1992).
3. R. P. Stanley, R. Houdré, U. Oesterle, *et al.*, Appl. Phys. Lett. **65**, 2093 (1994).
4. D. Baxter, M. S. Skolnick, A. Armitage, *et al.*, Phys. Rev. B **56**, 10032 (1997).
5. A. B. Pevtsov, A. V. Zherzdev, N. A. Feoktistov, *et al.*, Int. J. Electron. **78**, 289 (1995).
6. N. A. Feoktistov, N. L. Ivanova, L. E. Morozova, *et al.*, Mater. Res. Soc. Symp. Proc. **420**, 189 (1996).
7. A. A. Dukin, N. A. Feoktistov, V. G. Golubev, *et al.*, Appl. Phys. Lett. **77**, 3009 (2000).
8. V. G. Golubev, A. A. Dukin, A. V. Medvedev, *et al.*, Fiz. Tekh. Poluprovodn. (St. Petersburg) **35**, 1266 (2001) [Semiconductors **35**, 1213 (2001)].
9. A. A. Dukin, N. A. Feoktistov, V. G. Golubev, *et al.*, J. Non-Cryst. Solids **299–302**, 694 (2002).
10. A. Yariv and P. Yeh, *Optical Waves in Crystals* (Wiley, New York, 1984; Mir, Moscow, 1987).
11. G. Panzarini, L. C. Andreani, A. Armitage, *et al.*, Fiz. Tverd. Tela (St. Petersburg) **41**, 1337 (1999) [Phys. Solid State **41**, 1223 (1999)].
12. R. Ram, D. Babic, R. York, and J. Bowers, IEEE J. Quantum Electron. **31**, 399 (1995).

Translated by A. Sidorova